

Thermal X-ray iron line emission from the advection dominated accretion flow in the galactic binary GX 339-4

Ya-Di Xu

*Physics Department, Shanghai Jiao Tong University, 800 Dongchuan Road, Shanghai 200240, China;
Email: ydxu@sjtu.edu.cn*

ABSTRACT

We explore thermal X-ray iron line emission from the galactic X-ray binary GX 339-4 in the off state, using the models of the advection dominated accretion flow (ADAF) without or with outflows. The equivalent widths of hydrogen-like and helium-like thermal iron lines are calculated with different model parameters including viscosity parameter α , mass accretion rate at the outer radius of the ADAF \dot{m}_{out} and outflow strength parameter p . Our calculations show that the equivalent widths of thermal iron lines emitted from the pure ADAF, i.e., the ADAF without outflows, should be very small, assuming a solar metallicity for the accreting gas in the accretion flow. Strong thermal iron lines are expected to be emitted from the ADAF with relatively strong outflows. For reasonable choice of parameters, the total equivalent width of the He-like and H-like thermal iron lines reaches to $\gtrsim 500$ eV for accreting gas with solar metallicity. The observation of strong thermal X-ray lines from GX 339-4 at the off state may give a clue to the accretion mode of the source and provide evidence for the presence of outflows/winds in the accretion flow around the black hole in GX 339-4. It is found that the values of \dot{m}_{out} and p are degenerate, i.e., the observed X-ray continuum spectrum can be fairly well reproduced with different sets of the parameters \dot{m}_{out} and p . Such degeneracy can be broken when the thermal X-ray line emission data is available. We also compare our results with those in the previous similar work.

Subject headings: accretion, accretion disks black hole physics Stars: individual: GX 339-4 X-rays: stars

1. Introduction

The galactic X-ray binary (XRB) GX 339-4, one of the earliest proposed black hole candidates, has been attracted much attention after discovered in 1971 by the OSO-7 satellite (Markert et al. 1973). Based on the long-term broadband energy spectral observations, from the radio, infrared and optical, to the X-rays, GX 339-4 has been extensively studied on various issues (Fender et al. 1999; Corbel et al. 2000; Kong et al. 2000; Nowak et al. 2002; Miller et al. 2004, 2006; Dunn et al. 2008; Tomsick et al. 2008). Its spectral and temporal X-ray properties show a wide variety of canonical XRB states, transiting from off/quiescent state, low/hard state, intermediate state, high/soft state, and very high

state, but it spends most of its time in the low/hard state. A common argument is that the spectral states transitions are related to the changes of the mass accretion rate and the geometry of the accretion flow, though the physical mechanism of the changes are still quite uncertain (Narayan, Mahadevan & Quataert 1998; Done 2001).

Many different models were suggested to explain the observations of the different spectral states (see Narayan, Mahadevan & Quataert 1998; Done 2001, and references therein). The disk+corona models with different geometries, such as, an accretion disk corona (ADC) above or surrounded by a cold thin disk, or other similar geometries (see Nowak et al. 2002, for de-

tails and references therein), are used to interpret the observational features of the accretion flows around the black hole in different states. The observed X-ray spectra in different spectral states can be explained by the Comptonization (e.g., soft photons from the cold thin accretion disk are Comptonized in a hot corona) with different model parameters (Nowak et al. 2002; Corongiu et al. 2003). Narayan (1996) proposed that these different spectral states can be explained by outer thin disk plus inner advection dominated accretion flow (ADAF) models with varying accretion rate and transition radius (Esin et al. 1997, 1998). In this scenario, the transition radius increases with decreasing mass accretion rate \dot{m} ($\dot{m} = \dot{M}/\dot{M}_{\text{Edd}}$). There is a critical accretion rate \dot{m}_{crit} , above which the ADAF is suppressed and a standard thin disk is present in the inner region of the accretion flow. Miller et al. (2004, 2006) suggested that a standard thin disk may extend at or near to the innermost stable circular orbit (ISCO), at least in bright phases of the low/hard state, after fitting the spectra of GX 339-4 observed by Chandra during its decline of 2002-2003 outburst and by XMM-Newton during its 2004 outburst with a cool thin disk component and a relativistic Fe K line model. It is shown that the disk reflection model can also fit the spectra in the hard state when the total 1-100 keV luminosity even lower than $0.023L_{\text{Edd}}$ (Tomsick et al. 2008). Moreover, the presence of jet/outflow in the accretion flows has been explored to explain the radio emission and the radio/X-ray correlations in the low/hard state (Fender et al. 1999; Corbel et al. 2000; Markoff et al. 2003; Corbel et al. 2003).

Fluorescent Fe $K\alpha$ line emission is a very powerful trace of the inner edge (R_{in}) of the thin accretion disk around the black holes. Tomsick et al. (2009) used Suzaku and RXTE observations of GX 339-4 during 2008 to study the iron line profile at low luminosity state when the total 1-100 keV luminosity is $0.0014L_{\text{Edd}}$, and showed that the inner edge of the thin disk recedes and the truncated accretion disk is present around a black hole at low luminosity. If the ADAF exists in the inner region of the accretion flow as suggested by Narayan (1996), thermal X-ray iron lines may also emitted from the hot plasma in the ADAF surrounding the black hole at very low luminosity (Narayan & Raymond 1999; Perna et al.

2000; Xu et al. 2006; Xu & Cao 2009). It is shown that the average 0.4-12 keV X-ray flux that measured by RXTE between 2001 March and 2002 February and also on 2003 September 29 is $\sim 5.4 \times 10^{-12} \text{erg cm}^{-2} \text{s}^{-1}$, when GX 339-4 was in the quiescent state (Tomsick et al. 2009). This average flux corresponds to a luminosity of $L_X \simeq 4.2 \times 10^{34} \text{erg s}^{-1} \sim 3.2 \times 10^{-5} L_{\text{Edd}}$, if we adopt values of $m = 10$ ($m = M/M_{\odot}$) and $d = 8$ kpc for GX 339-4. Chandra even detected a 0.4-11 keV flux of $3.8 \times 10^{-13} \text{erg cm}^{-2} \text{s}^{-1}$ on 2003 September 29 (Gallo et al. 2003), which is more than an order of magnitude lower than the average quiescent value above. In such very low luminosity quiescent states, the accretion rate is much lower than the critical accretion rate \dot{m}_{crit} , the outer thin disk may be suppressed, and the temperature of the plasma in the outer region of the ADAF may be low to $T_e \sim 10^{7-8} \text{K}$, so the He-like (Fe XXV) and H-like (Fe XXVI) thermal X-ray iron lines centered at energy ~ 6.7 keV and ~ 6.97 keV, respectively, can be produced in this region of the ADAF. Narayan & Raymond (1999) calculated the thermal X-ray line emission including He-like and H-like iron lines from another X-ray binary, V404 Cyg, in quiescence with the ADAF models with and without winds, and concluded that an ADAF with a large outer radius would produce reasonably strong thermal iron lines if winds are present in the source. However, for the ADAF models with winds, the dynamical structure of the ADAFs are solved based on some simplified assumptions in Narayan & Raymond (1999). In this work, we will use the improved numerical approach to derive the global two-temperature structures of the ADAF models by solving the full relativistic hydrodynamical equations with the modeling techniques suggested by Manmoto (2000), in which all the radiation processes are included.

In this work, we model the thermal X-ray iron line emission from the galactic X-ray binary GX 339-4 in the off state, using the advection dominated accretion flow (ADAF) models with or without outflows (Blandford & Begelman 1999). The models are constrained by the Chandra's observed X-ray continuum, the power-law photon index of 2 ± 0.2 and the integrated 0.4-11 keV flux of $3.8 \times 10^{-13} \text{erg cm}^{-2} \text{s}^{-1}$ (Gallo et al. 2003). We describe the calculation of dynamical structures of

the ADAF in §2. The calculation of the equivalent widths of the thermal X-ray iron line emission is described in §3. The results are shown in §4. In §5., we discuss the results and the physical implications of the results, and compare our results of V404 Cyg with those in Narayan & Raymond (1999).

2. Dynamical structures of the ADAF models

We employ the approach suggested by Manmoto (2000) to calculate the global structure of an accretion flow surrounding a Schwarzschild black hole in the general relativistic frame. All the radiation processes are included in the calculations of the global accretion flow structure (see Manmoto 2000; Yuan et al. 2009, for details and the references therein). In this work, we include outflows in the calculation of the ADAF structure, which have not been considered by Manmoto (2000), and the values of some parameters adopted in this work are different from those in Manmoto (2000).

The global structure of an accretion flow surrounding a black hole with mass M_{bh} can be calculated, if some parameters \dot{m} , α , β and δ are specified. The value of the viscosity parameter α is still a controversial issue. Narayan (1996) assumed a fairly large value, $\alpha = 1$, in order to reproduce the maximum luminosities observed in low-state XRBs, while Esin et al. (1997) suggested a smaller value, $\alpha = 0.25$, in their spectral model calculations. Recently, the influence of viscosity parameter α on the transition luminosity between the spectral states of accreting X-ray binaries was explored with a wide range of α from 0.1 to 0.9 (Qiao & Liu 2009), which shows that the detected transition luminosity between the spectral states of many galactic accreting X-ray binaries can be fitted by tuning the value of α . In this work, we adopt two different values of $\alpha = 0.2$ and 0.5 in the calculations, respectively. The parameter β , defined as $p_{\text{m}} = B^2/8\pi = (1 - \beta)p_{\text{tot}}$, ($p_{\text{tot}} = p_{\text{gas}} + p_{\text{m}}$), describes the magnetic field strength of the accretion flow. We assume $\beta = 0.8$ in all the calculations. This parameter will mainly affect the radio spectrum from the source, while it has little effect on the X-ray emission, which we mostly focus on in this work. The parameter δ describes the fraction of the viscously dissipated energy di-

rectly going into electrons in the accretion flow. It was pointed out that a significant fraction of the viscously dissipated energy could go into electrons by magnetic reconnection, if the magnetic fields in the flow are strong (Bisnovatyi-Kogan & Lovelace 1997, 2000). The value of δ is still uncertain, and we adopt a conventional value of $\delta = 0.1$ in all the calculations as that adopted in Cao (2007).

In this work, the global two-temperature structures of the ADAF models are derived numerically by solving the full relativistic hydrodynamical equations under the modeling techniques suggested by Manmoto (2000). The main improvements of this solution compared with the previous works (e.g., Gammie & Popham 1998) are that the advected fraction of the dissipated energy f in the energy equations is not treated as a parameter and the detailed radiation processes including synchrotron, comptonization, and bremsstrahlung are calculated self-consistently. Although Manmoto (2000) found that the solution with $f = 1$ is quite identical with the solution obtained by fully solving the energy equations, especially in the innermost part of the flow, there is a difference in the surface density in the outer region of the ADAF (see Figure 4 in Manmoto 2000), which is the dominant region contributing to the thermal X-ray iron line emissions we explored in this work. In Narayan & Raymond (1999), the advected fraction of the dissipated energy f is assumed to be a constant in solving the global structures of the ADAFs (Quataert & Narayan 1999; Gammie & Popham 1998; Esin et al. 1997), and the continuum emissions from the ADAFs are computed using the solved global structures of the ADAFs. Moreover, they have not calculated the global structure of the ADAFs with winds, instead, they simply adopted the radial velocity, angular velocity, and sound speed of the flow derived from the global relativistic models of Gammie & Popham (1998) under the assumption of a constant mass accretion rate. The density of the accretion flow is then calculated by applying the continuity equation with a variable r -dependent mass accretion rate (see Quataert & Narayan 1999, for the details).

Given the values for parameters α , β and δ , the mass accretion rate \dot{m} can be tuned to fit the observed X-ray continuum spectrum when the outer radius of ADAF is fixed. In low-mass

BHXBs, where mass is transferred via Roche lobe overflow, the circularization radius of the incoming stream is large ($R_{\text{circ}} \sim 10^4 - 10^5 R_S$, $R_S = 2GM/c^2$) (Esin et al. 1997). We assume the dimensionless outer radius of the ADAF surrounding the black hole in GX 339-4 to be $r_{\text{out}} = R_{\text{out}}/R_S = 5 \times 10^4$ in our calculations. A constant mass accretion rate \dot{m} independent of radius is adopted for the pure ADAF model. The jet/outflow models were widely used to account for the observed broadband spectra and the radio/X-ray correlations of GX 339-4 and other X-ray binaries in the low or off state, though the origin of the outflows in the accretion flows is still unclear (Corongiu et al. 2003; Markoff et al. 2001, 2003; Tomsick et al. 2008). In this work, we employ a power-law r -dependent mass accretion rate,

$$\dot{m} = \dot{m}_{\text{out}}(r/r_{\text{out}})^p, \quad (1)$$

to describe the outflows from the ADAF, where the power-law index p represents the strength of the outflows in the accretion flow, and \dot{m}_{out} is the mass accretion rate at the outer radius. It can be easily found that the pure ADAF model is a specific case of ADAF with outflows model for $p = 0$. The global structure of the ADAF is calculated, and then the spectrum is derived to reproduce the observed X-ray continuum by tuning the values of \dot{m}_{out} and p .

3. Calculations of line equivalent widths

Based on the structure of the ADAF calculated as described in the last section, we can compute the thermal X-ray iron line emission from GX 339-4. The equivalent width of an emission line is defined as

$$\text{EW}_{\text{line}} = L_{\text{line}}/L_{\nu}(\nu_{\text{line}}), \quad (2)$$

where L_{line} is the total luminosity of the emission line, and $L_{\nu}(\nu_{\text{line}})$ is the spectral luminosity of the continuum at the energy of the line ν_{line} . The total line luminosity L_{line} is available by integrating the emission from the hot gas over the different shells of the accretion flow,

$$L_{\text{line}} = \int_{r_{\text{in}}}^{r_{\text{out}}} n_e^2(r) \epsilon_{\text{line}}(T_e) 4\pi r H dr R_S^2, \quad (3)$$

where n_e is the electron density at dimensionless radius $r = R/R_S$, $r_{\text{in}} = R_{\text{in}}/R_S$ and $r_{\text{out}} =$

R_{out}/R_S are the inner and outer radii of the accretion flow. The density n_e and the vertical half thickness H of the ADAF as functions of radius are given by the derived global ADAF structure. The quantity ϵ_{line} is the line emissivity for unit density of plasma at a certain radius, which is a function of the local electron temperature.

Given the electron temperature of the plasma, we use the standard software package Astrophysical Plasma Emission Code (APEC) (Smith et al. 2001) to calculate the emissivity of the chosen line. We assume a solar abundance and ionization equilibrium in the calculations. Perna et al. (2000) found that departures from ionization equilibrium were small in a model with $\alpha=0.1$, but they will be more severe in the models with larger values of α adopted here. The APEC code includes collisional excitation, recombination to excited levels and dielectronic satellite lines. It ignores photoionization, which is a few percent effect at most (Narayan & Raymond 1999). The spectral continuum luminosity $L_{\nu}(\nu_{\text{line}})$ from the accretion flow is calculated with the derived ADAF structure. We compute the He-like and H-like line equivalent widths of iron, EW_1 and EW_2 , centered at energy ~ 6.7 keV and ~ 6.97 keV, respectively. The solar metallicity Z_{\odot} is adopted in the calculations. The results can be scaled to other metallicities Z using

$$\text{EW}_{1,2}(Z) = \frac{Z}{Z_{\odot}} \text{EW}_{1,2}(Z_{\odot}). \quad (4)$$

4. Results

The system parameters (and companion star) of GX 339-4 have not been directly measured. Hynes et al. (2003) estimated a 1.7557 days orbital period by analyzing the observed NIII (Bowen blend) lines and He II wings, and derived a minimum mass of $5.8M_{\odot}$ for the black hole in GX 339-4. The distance of GX 339-4 is estimated to be $d \gtrsim 6$ kpc from the optical Na D line profiles, and perhaps even to be as large as 15 kpc (Hynes et al. 2004). Zdziarski et al. (2004) estimated the distance to be $\gtrsim 7$ kpc based on Very Large Telescope (VLT) observation of GX 339-4. We adopt $M = 10M_{\odot}$ and $d = 8$ kpc in all the calculations, which are the same as those adopted in Tomsick et al. (2009).

As discussed in §2, most of the disk parameters

are fixed in the calculations of the global structure of the ADAFs, except the viscosity parameter α , the parameter p describing the strength of the outflows, and the mass accretion rate at the outer radius of the ADAF \dot{m}_{out} . The calculations are carried out with different viscosity parameters, $\alpha = 0.2$ and $\alpha = 0.5$, respectively. The calculated global structures of some ADAFs with different parameters are plotted in Figures 1 and 2.

Based on the derived ADAF structure, the continuum spectrum can be calculated (see Cao 2005, 2007, for the details). The value of the mass accretion rate at the outer radius of the ADAF \dot{m}_{out} and the outflow strength parameter p are tuned in order to fit the observed X-ray continuum spectrum between 0.4-11 keV (Gallo et al. 2003). It is found that the values of \dot{m}_{out} and p are degenerate, i.e., the X-ray continuum spectrum can be fairly well reproduced with different sets of the parameters \dot{m}_{out} and p (see Figure 3).

Assuming a solar metallicity for the plasmas in the ADAF, we calculate the equivalent widths of the thermal He-like and H-like iron lines emitted from the accretion flows as described in §3. The results are listed in Table 1, where $\text{EW}_1(Z_\odot)$ and $\text{EW}_2(Z_\odot)$ represent the equivalent widths of the thermal He-like and H-like iron lines, respectively. The adopted parameters are also shown in Table 1. The total equivalent widths of the He-like and H-like iron lines emitted from the ADAFs surrounding the black hole in GX 339-4 are plotted in Figure 4 as a function of the outer mass accretion rate for the models with different strength of the outflow. The results show that the predicted EWs of the He-like and H-like iron lines from the pure ADAFs are too small to be observed. For the ADAFs with outflows, the EWs of the thermal iron lines significantly increase with the strength of the outflow.

5. Discussion

In this paper we have explored the thermal X-ray line emission from the accretion flow surrounding the black hole in the galactic binary GX 339-4. We construct the ADAF models for the observed X-ray spectrum of GX 339-4 with different parameters including the viscosity parameter α , the mass accretion rate \dot{m} and the outflow strength p . We compute the equivalent widths of the helium-like

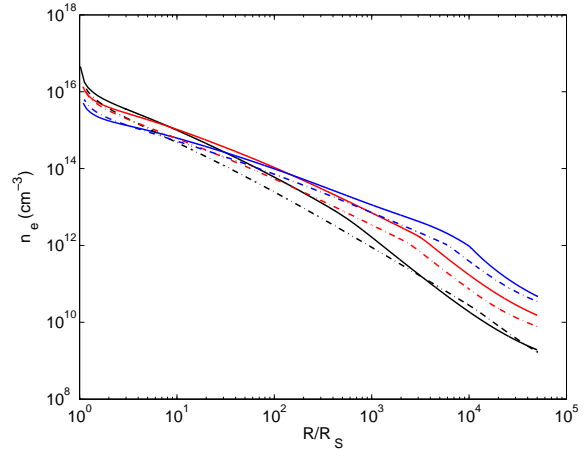


Fig. 1.— Electron density distributions of the ADAF models with $\alpha = 0.2$ and $\alpha = 0.5$, respectively. The black solid line corresponds to the pure ADAF model with parameters $\alpha = 0.2$, $\dot{m} = 0.001$. The red and blue solid lines correspond to the ADAF with outflows models with parameters $\alpha = 0.2$, $\dot{m}_{\text{out}} = 0.008$, $p = 0.25$, and $\alpha = 0.2$, $\dot{m}_{\text{out}} = 0.025$, $p = 0.45$, respectively. The black dot-dashed line corresponds to the pure ADAF model with parameters $\alpha = 0.5$, $\dot{m} = 0.001$. The red and blue dot-dashed lines correspond to the ADAF with outflows models assuming parameters $\alpha = 0.5$, $\dot{m}_{\text{out}} = 0.01$, $p = 0.25$, and $\alpha = 0.5$, $\dot{m}_{\text{out}} = 0.045$, $p = 0.45$, respectively.

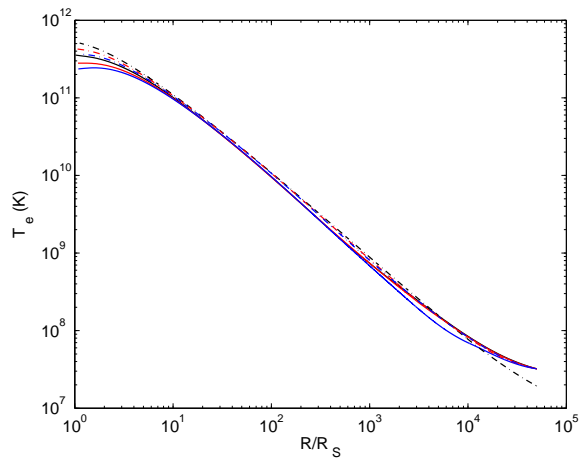


Fig. 2.— Same as Figure 1, but for the electron temperature distributions.

TABLE 1

EQUIVALENT WIDTHS $EW_1(Z_\odot)$ AND $EW_2(Z_\odot)$ IN UNITS OF eV OF THE THERMAL HELIUM-LIKE AND HYDROGEN-LIKE X-RAY IRON LINES FROM THE ADAFs

α	\dot{m}_{out}	p	$EW_1(\text{eV})$	$EW_2(\text{eV})$
0.2	0.001	0.	0.7	0.7
0.2	0.008	0.25	28.9	24.3
0.2	0.01	0.3	54.5	41.1
0.2	0.015	0.35	103.9	69.0
0.2	0.02	0.4	196.2	110.1
0.2	0.025	0.45	368.0	169.2
0.5	0.001	0.	0.4	0.5
0.5	0.01	0.25	7.4	6.5
0.5	0.015	0.3	17.0	13.6
0.5	0.025	0.35	38.8	27.5
0.5	0.035	0.4	77.2	48.2
0.5	0.045	0.45	141.0	77.1

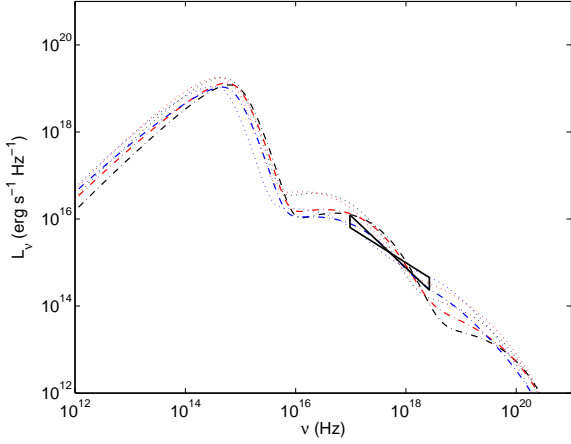


Fig. 3.— Spectra of ADAF models with $\alpha = 0.2$ and $\alpha = 0.5$, respectively. The black dotted line corresponds to the pure ADAF model with parameters $\alpha = 0.2$, $\dot{m} = 0.001$. The red and blue dotted lines correspond to the ADAF with outflows models with parameters $\alpha = 0.2$, $\dot{m}_{\text{out}} = 0.008$, $p = 0.25$, and $\alpha = 0.2$, $\dot{m}_{\text{out}} = 0.025$, $p = 0.45$, respectively. The black dot-dashed line corresponds to the pure ADAF model with parameters $\alpha = 0.5$, $\dot{m} = 0.001$. The red and blue dot-dashed lines correspond to the ADAF with outflows models assuming parameters $\alpha = 0.5$, $\dot{m}_{\text{out}} = 0.01$, $p = 0.25$, and $\alpha = 0.5$, $\dot{m}_{\text{out}} = 0.045$, $p = 0.45$, respectively. The black tie represents the observed 0.4-11 keV X-ray spectrum from Gallo et al. (2003).

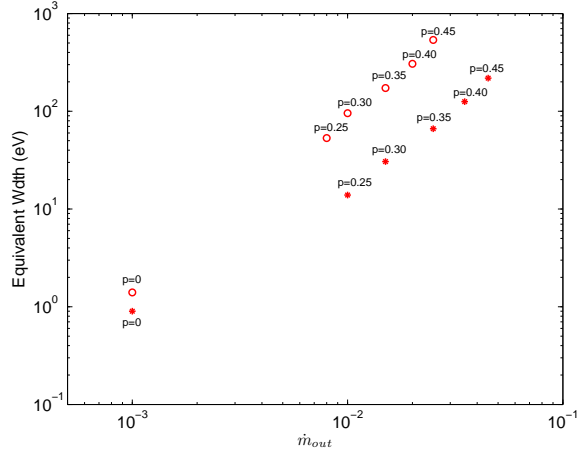


Fig. 4.— Total equivalent widths of the He-like and H-like iron lines from the ADAFs as a function of the outer mass accretion rate. Circles and stars represent the data for models with $\alpha = 0.2$ and $\alpha = 0.5$, respectively. The power-law indexes, p , in Equation (1) are indicated in the figure for different ADAF models, while $p = 0$ corresponds to the pure ADAF models.

and hydrogen-like thermal iron lines from the accretion flows.

From Table 1 and Figure 4, we can see that the thermal X-ray line emission from the ADAFs without outflows is always much lower than emission from the ADAFs with outflows. Moreover, the equivalent widths of the He-like and H-like thermal iron lines significantly increase with the mass accretion rate \dot{m}_{out} at the outer radius of the ADAF and the outflow strength parameter p . In fact, these two parameters are not independent, i.e., the outflow strength parameter p is required to increase with the mass accretion rate \dot{m}_{out} at the outer radius to reproduce the observed X-ray continuum spectrum. The sensitive dependence of EW_1 and EW_2 on the two parameters can be explained by the very different density profiles (see Figure 1), because the temperature profiles of the plasmas are quite similar for ADAFs with different parameters adopted (see Figure 2, and Narayan & Yi 1995). As showed in Equation (2), the equivalent width of a thermal line is the ratio of the line luminosity and the spectral luminosity at the energy of the line. All our derived spectra are required to fit the observed X-ray continuum at ~ 6.83 keV. Thus, the equivalent widths of thermal iron lines will mainly depend on the line luminosities. From Equation (3), the line luminosity emitted from a certain annulus of the accretion flow is determined by the density and the line emissivity, which is a function of the electron temperature. As the temperature profiles are quite similar for the models with different parameters, the line luminosity is mostly determined by the density distribution of the gas in the accretion flow. For the models with larger p , i.e., stronger outflows, the density profiles are flatter, which means that much more gases are blown away from the accretion flow. This leads to higher electron densities in the outer region of the accretion flow ($r \gtrsim 10^3$) with the electron temperature $\lesssim 10^8$ K, where the thermal He-like and H-like iron lines emitted. Therefore, the line luminosity and the equivalent widths of the thermal iron lines are higher in these models.

The change of the equivalent widths of the thermal iron lines emitted from the ADAFs with the value of the viscosity parameter α is explored in this work. Comparing the two groups of the line equivalent widths for different values of viscosity,

$\alpha = 0.2$ and $\alpha = 0.5$, we find that the EWs of the lines from the ADAFs with $\alpha = 0.2$ are always larger than those from the ADAFs with $\alpha = 0.5$ if the same value of p , i.e., strength of the outflows, is adopted. This is because the larger the viscosity is, the quicker the gas flows in, which leads to smaller densities of the gas in the outer region of the ADAF (see Figure 1).

We theoretically conclude in this work that the galactic X-ray binary GX 339-4 may produce X-ray iron lines with very large equivalent width in the quiescence. For reasonable choice of model parameters, e.g., $\alpha = 0.2$, $\dot{m}_{\text{out}} = 0.25$ and $p = 0.45$, the total equivalent width of the He-like and H-like iron lines from the ADAFs with moderately strong outflows reaches to $\gtrsim 500$ eV, when the 0.4-11 keV X-ray flux is about $3.8 \times 10^{-13} \text{erg cm}^{-2} \text{s}^{-1}$. If these strong thermal lines are really observed, it may give a clue to the accretion mode of the source in the off state and provide strong evidence that the outflows/winds exist in GX 339-4. In fact, Feng et al. (2001) showed that a prominent thermal X-ray iron line, with the equivalent width of 595_{-172}^{+248} eV and the line energy centered at $6.83_{-0.16}^{+0.16}$ keV, is present in the RXTE (PCA) observation of GX 339-4 in 1999 when the source is in the off state with the integrated 3-20 keV flux of $7 \times 10^{-12} \text{erg cm}^{-2} \text{s}^{-1}$. However, we need to bear in mind that the observation with RXTE may include possible contamination from the Galactic ridge or other sources. Observations with ASCA, Suzaku and Chandra have detected an iron line emission at 6.7 keV and suggested it to be emitted by the diffuse hot plasma and/or produced by point sources (see, e.g., Koyama et al. 1986; Tanaka 2002; Revnivtsev et al. 2009). Thus, we select the Chandra observation (Gallo et al. 2003) as the quiescence flux in our calculations.

Due to the different sources we explored and different parameters we used in the calculations, it is not easy to directly compare the equivalent widths of thermal iron lines from GX 339-4 derived in this work with those from V404 Cyg predicted by Narayan & Raymond (1999). Therefore, we recalculate the equivalent widths of the thermal iron lines emitted from V404 Cyg in quiescence with our ADAF model for the same model parameters as those used in Narayan & Raymond (1999). The comparison of the results is shown in Table 2. The value of parameter β in Narayan & Raymond

(1999) (defined as $\beta = p_{\text{gas}}/p_{\text{mag}}$) has been translated to the value with the definition in this work. The equivalent width of the He-like iron line EW_1 of Narayan & Raymond (1999) is the sum of the several He-like lines with the energy between 6.65 keV and 6.75 KeV which can be compared with the result of this work, because we have already combined the equivalent widths of He-like lines near the energy of 6.7 keV in bins of 100 eV width which we believe to be more comparable with the observation. Moreover, we note that the equivalent width of the H-like iron line of Narayan & Raymond (1999) only includes one line Fe XXVI $\lambda 1.780$ while the data of this work is also the sum of the H-like lines in bins of 100 eV width, i.e. with the energy between 6.92 keV and 7.02 keV. The emission in the 100 eV bin is larger than that of the line calculated by Narayan & Raymond (1999). The calculated X-ray continuum derived from the approach of this work is a bit larger than the ASCA observation of V404 Cyg (Narayan et al. 1997) if the same mass accretion rate \dot{m}_{out} as Narayan & Raymond (1999) is adopted. Using the same model parameters δ, α, β and the strength of the wind p as Narayan & Raymond (1999), our calculation shows that the best fitted mass accretion rate is $\dot{m}_{\text{out}} = 0.004$ (the results are listed in Table 2). The discrepancy of the results between this work and Narayan & Raymond (1999) is significant, which is mainly due to the difference of ADAF structure calculations.

We thank the anonymous referee for very helpful suggestions. This work is supported by the NSFC (grants 10778621, 10703003, and 11078014).

REFERENCES

- Bisnovatyi-Kogan G. S., & Lovelace R. V. E. 1997, ApJ, 486, L43
- Bisnovatyi-Kogan G. S., Lovelace R. V. E., 2000, ApJ, 529, 978
- Blandford, R. D., & Begelman, M. C. 1999, MNRAS, 303, L1
- Cao, X. 2005, ApJ, 631, L101
- Cao, X. 2007, ApJ, 659, 950
- Corbel, S., Fender, R. P., Tzioumis, A. K., Nowak, M., McIntyre, V., Durouchoux, P., & Sood, R. 2000, A&A, 359, 251
- Corbel, S., Nowak, M. A., Fender, R. P., Tzioumis, A. K., & Markoff, S. 2003, A&A, 400, 1007
- Corongiu, A., Chiappetti, L., Haardt, F., Treves, A., Colpi, M., & Belloni, T. 2003, A&A, 408, 347
- Done, C. 2001, Advances in Space Research, 28, 255
- Dunn, R. J. H., Fender, R. P., Körding, E. G., Cabanac, C., & Belloni, T. 2008, MNRAS, 387, 545
- Esin, A. A., McClintock, J. E., & Narayan, R. 1997, ApJ, 489, 865
- Esin, A. A., Narayan, R., Cui, W., Grove, J. E., & Zhang, S.-N. 1998, ApJ, 505, 854
- Fender, R., et al. 1999, ApJ, 519, L165
- Feng, Y. X., Zhang, S. N., Sun, X., Durouchoux, P., Chen, W., & Cui, W. 2001, ApJ, 553, 394
- Gallo, E., Fender, R., & Corbel, S. 2003, The Astronomer's Telegram, 196, 1
- Gammie, C. F., & Popham, R. 1998, ApJ, 498, 313
- Hynes, R. I., Steeghs, D., Casares, J., Charles, P. A., & O'Brien, K. 2003, ApJ, 583, L95
- Hynes, R. I., Steeghs, D., Casares, J., Charles, P. A., & O'Brien, K. 2004, ApJ, 609, 317
- Kong, A. K. H., Kuulkers, E., Charles, P. A., & Homer, L. 2000, MNRAS, 312, L49
- Koyama, K., Makishima, K., Tanaka, Y., & Tsunemi, H. 1986, PASJ, 38, 121
- Manmoto, T. 2000, ApJ, 534, 734
- Markert, T. H., Canizares, C. R., Clark, G. W., Lewin, W. H. G., Schnopper, H. W., & Sprott, G. F. 1973, ApJ, 184, L67
- Markoff, S., Falcke, H., & Fender, R. 2001, A&A, 372, L25

TABLE 2

COMPARISON OF THE EQUIVALENT WIDTHS $EW_1(Z_\odot)$ AND $EW_2(Z_\odot)$ OF THE THERMAL HELIUM-LIKE AND HYDROGEN-LIKE X-RAY IRON LINES FROM V404 CYG CALCULATED BY THE SOLUTIONS IN THIS WORK AND IN NARAYAN & RAYMOND (1999)

Data	δ	α	β	p	\dot{m}_{out}	$EW_1(\text{eV})$	$EW_2(\text{eV})$
NY99 ⁽¹⁾	0.3	0.1	0.91	0.4	0.006	230	79 ⁽²⁾
this work	0.3	0.1	0.91	0.4	0.006	182	113
this work	0.3	0.1	0.91	0.4	0.004	122	79

NOTE.—(1) NY99 represents the data from Narayan & Raymond (1999). (2) EW_2 of Narayan & Raymond (1999) includes only one line Fe XXVI $\lambda 1.780$ while the data of this work is the sum of the H-like iron lines in bins of 100 eV width, i.e. with the energy between 6.92 keV and 7.02 keV.

- Markoff, S., Nowak, M., Corbel, S., Fender, R., & Falcke, H. 2003, *A&A*, 397, 645
- Miller, J. M., et al. 2004, *ApJ*, 601, 450
- Miller, J. M., Homan, J., Steeghs, D., Rupen, M., Hunstead, R. W., Wijnands, R., Charles, P. A., & Fabian, A. C. 2006, *ApJ*, 653, 525
- Narayan, R. 1996, *ApJ*, 462, 136
- Narayan, R., Barret, D., & McClintock, J. E. 1997, *ApJ*, 482, 448
- Narayan, R., Mahadevan, R., & Quataert, E. 1998, in *Theory of Black Hole Accretion Disks*, ed. M. A. Abramowicz, G. Björnsson, & J. E. Pringle
- Narayan, R., & Raymond, J. 1999, *ApJ*, 515, L69
- Narayan, R., & Yi, I. 1995, *ApJ*, 452, 710
- Nowak, M. A., Wilms, J., & Dove, J. B. 2002, *MNRAS*, 332, 856
- Perna, R., Raymond, J., & Narayan, R. 2000, *ApJ*, 541, 898
- Qiao, E., & Liu, B. F. 2009, *PASJ*, 61, 403
- Quataert, E., & Narayan, R. 1999, *ApJ*, 520, 298
- Revnivtsev, M., Sazonov, S., Churazov, E., Forman, W., Vikhlinin, A., & Sunyaev, R. 2009, *Nature*, 458, 1142
- Smith, R. K., Brickhouse, N. S., Liedahl, D. A., & Raymond, J. C. 2001, *ApJ*, 556, L91
- Tanaka, Y. 2002, *A&A*, 382, 1052
- Tomsick, J. A., et al. 2008, *ApJ*, 680, 593
- Tomsick, J. A., Yamaoka, K., Corbel, S., Kaaret, P., Kalemci, E., & Migliari, S. 2009, *ApJ*, 707, L87
- Xu, Y.-D., Narayan, R., Quataert, E., Yuan, F., & Baganoff, F. K. 2006, *ApJ*, 640, 319
- Xu, Y.-D., & Cao, X.-W. 2009, *Res. Astron. Astrophys.*, 9, 401
- Yuan, Y.-F., Cao, X., Huang, L., & Shen, Z.-Q. 2009, *ApJ*, 699, 722
- Zdziarski, A. A., Gierliński, M., Mikołajewska, J., Wardziński, G., Smith, D. M., Harmon, B. A., & Kitamoto, S. 2004, *MNRAS*, 351, 791

This 2-column preprint was prepared with the AAS L^AT_EX macros v5.2.